Cardiovascular Research (2008) **80**, 416–424
doi:10.1093/cvr/cvn215

Inhibition of class I histone deacetylase with an apicidin derivative prevents cardiac hypertrophy and failure

Pasquale Gallo[1,2†], Michael V.G. Latronico[3†], Paolo Gallo[1,4], Serena Grimaldi[3], Francesco Borgia[5], Matilde Todaro[6], Philip Jones[2], Paola Gallinari[2], Raffaele De Francesco[2], Gennaro Ciliberto[2], Christian Steinkühler[2], Giovanni Esposito[5], and Gianluigi Condorelli[3,7*]

[1]*Laboratory of Molecular Cardiology, San Raffaele Science Park Foundation, Rome, Italy;* [2]*Istituto di Ricerche di Biologia Molecolare P. Angeletti, IRBM-Merck Research Laboratories Rome, Pomezia, Italy;* [3]*Laboratory of Genetic and Molecular Cardiology, Scientific and Technology Pole, IRCCS MultiMedica, Milan, Italy;* [4]*Campus Bio-Medico di Roma, Rome, Italy;* [5]*Division of Cardiology, Federico II University, Naples, Italy;* [6]*Department of Surgical and Oncological Sciences, University of Palermo, Palermo, Italy; and* [7]*Division of Cardiology, Department of Medicine, University of California San Diego, 9500 Gilman Drive, BSB 5022, La Jolla, CA 92093-0613, USA*

Received 28 November 2007; revised 24 July 2008; accepted 29 July 2008; online publish-ahead-of-print 12 August 2008

Time for primary review: 29 days

KEYWORDS
Hypertrophy;
Heart failure;
Histone deactylase inhibitors

Aims Recent studies have demonstrated the importance of chromatin remodelling via histone acetylation/deacetylation for the control of cardiac gene expression. Specific histone deacetylases (HDACs) can, in fact, play a positive or negative role in determining cardiac myocyte (CM) size. Here, we report on the effect on hypertrophy development of three inhibitors (HDACi) of class I HDACs.
Methods and results The compounds were first analysed *in vitro* by scoring hypertrophy, expression of foetal genes, and apoptosis of neonatal rat CMs stimulated with phenylephrine, an α1-adrenergic agonist. This initial screening indicated that a truncated derivative of apicidin with class I HDAC specificity, denoted API-D, had the highest efficacy to toxicity ratio, and was thus selected for further analysis *in vivo*. Administration of this drug significantly decreased myocardial hypertrophy and foetal gene expression after 1 week of pressure overload induced by thoracic aortic constriction (TAC) in mice. After 9 weeks of TAC, when manifest heart failure is encountered, mice treated with API-D presented with significantly improved echocardiographic and haemodynamic parameters of cardiac function when compared with untreated TAC-operated mice.
Conclusion The apicidin derivative, API-D, is capable of reducing hypertrophy and, consequently, the transition to heart failure in mice subjected to TAC. Treatment with this substance, therefore, holds promise as an important therapeutic option for heart failure.

1. Introduction

Histone deacetylases (HDACs) remodel chromatin in a gene-specific fashion by changing nucleosomal packaging of DNA: deacetylation of histones H3 and H4 by HDACs inhibits transcription, whereas their acetylation by histone acetyltransferases (HATs) results in transcriptional activation.[1] HDACs, thus, can regulate important cellular functions through gene expression control. In particular, regulation of histone acetylation is implicated in proper cell function, differentiation, and cell growth.[2,3] The pharmacological inhibition of HDACs has, therefore, raised significant interest in the pharmaceutical industry particularly in the search for new anti-proliferative molecules.

Mammalian HDACs can be divided into four classes based on their sequence motifs and catalytic mechanisms.[4,5] Class I, II, and IV HDACs are evolutionarily related Zn^+-dependent hydrolases. The members of class I (HDAC1, -2, -3, and -8) are expressed ubiquitously and consist mainly of a deacetylase domain. Class II HDACs (HDAC4, -5, -7, and -9) are highly expressed in muscle, brain, and T cells. They have an extended N-terminus, which serves as a target for protein–protein interactions and for post-translational modifications, such as phosphorylation, important for their function and governing nuclear-cytoplasmic shuttling.[6] HDAC11 is considered to be structurally diverse enough from the other Zn^+-dependent HDACs to be classified as a separate class (class IV).[7] Class III HDACs are related to the yeast HDAC, silent information regulator 2, and use nicotinamide adenine dinucleotide as a co-substrate.[8]

With regard to myocardial hypertrophy, studies have demonstrated that HDACs suppress this process.[9,10] Moreover,

† These authors contributed equally to the work.
*Corresponding author. Tel: +1 858 822 5010; fax: +1 858 822 3027.
E-mail address: gcondorelli@ucsd.edu

inhibition of general HDAC activity has also been reported to suppress hypertrophy.[11,12] It was suggested that different classes of HDACs suppress distinct sets of hypertrophic program-influencing genes. For example, whereas class II HDACs suppress pro-hypertrophic genes, class I HDACs might repress expression of anti-hypertrophic genes. If the anti-hypertrophic gene products were dominant over the genes suppressed by class II HDACs, one would expect HDAC inhibitors to block hypertrophy. Accordingly, inhibition of class I HDACs would result in a de-repression of such anti-hypertrophic genes and consequently block hypertrophy. There is evidence for a potential role of class I HDACs in cardiac growth, but the mechanism is still undefined and even less clear than for class II HDACs.[13,14]

In addition, evidence from rodent models indicates that cardiac function is preserved when hypertrophy is inhibited in the face of stress signalling. This points to the potential importance of therapeutic strategies that modulate the hypertrophic process.[15–22]

In the present study, we have defined the binding specificity of novel HDAC inhibitors (HDACis) and have evaluated the role of specific inhibitors of class I HDACs in the prevention of cardiac hypertrophy *in vitro* and *in vivo*. Our data suggest that class I HDAC inhibition has potential use in heart failure.

2. Methods

2.1 *In vitro* histone deacetylase inhibition assays

C-terminally flag-tagged HDAC1, -2, -3, -6, -9, and -11 were expressed in HEK293 cells, affinity purified using anti-flag antibody affinity resin, and eluted with a 3X flag peptide. HDAC4, -5, -7, and -8 were expressed in *Escherichia coli*. The obtained molecules were then purified to apparent homogeneity [Coomassie-stained sodium dodecyl sulphate polyacrylamide gel electrophoresis (SDS–PAGE)] by nickel affinity then anion-exchange (MonoQ) chromatographies, and finally, by gel filtration. IC_{50} values of the inhibitor molecules were then determined using the HDAC Fluorescent Activity Assay (BioMol Research Laboratories).

2.2 Histone deacetylase inhibitors

Three HDAC inhibitors, MS27-275, PXD-101, and API-D, were chosen based on suitable pharmacokinetic properties and bioavailability for *in vivo* studies. MS27-275 is an aminobenzamide[23] with selectivity for HDAC1, -2, and -3 when assayed on a panel of purified HDAC subtypes. PXD-101 belongs to the hydroxamic acid class of inhibitors[24] and inhibits both class I and class II enzymes, albeit with different potencies. The third inhibitor, API-D, is a derivative of the cyclic peptide, apicidin, a structurally novel HDAC inhibitor;[25] it also shows selectivity for HDAC class I subtypes 1, 2, and 3 (*Table 1*).

2.3 *In vitro* experimentation

Cardiomyocytes (CMs) were obtained as previously described from 3-day-old neonatal Wistar rat pups (Charles River Laboratories).[26] CMs were seeded on gelatin-coated plates and kept overnight in medium containing 15% serum to which mitomycin (Sigma) had been added to inhibit overgrowth of non-cardiomyocytes. Cultures contained <95% CMs as assessed by immunofluorescence for cardiac troponin I (Chemicon). The morning following seeding, CMs were washed, treated with HDACi and/or phenylephrine (PE), and assayed as described later.

Table 1 IC_{50} data (nM) of the histone deacetylase (HDAC) inhibitors for single class I, II, and IV HDACs

Class	HDAC	MS27–275	PXD-101	API-D
I	1	171	57	13
	2	421	88	18
	3	337	25	11
	8	28 780	56	>1000
II	4	>50 000	4581	>1000
	5	>50 000	7018	>1000
	6	>50 000	40	680
	7	>50 000	2008	>1000
	9	n.d.	n.d.	n.d.
	10	n.d.	n.d.	n.d.
IV	11	>50 000	19 540	n.d.

Values are means of three or more experiments. n.d., not determined.

2.3.1 Treatment with histone deacetylase inhibitors and induction of hypertrophy

The morning following seeding, CMs were washed in phosphate buffered saline (PBS) and pre-treated in serum-free medium containing HDACi at the indicated doses. A medium change was done 24 h later, again with serum-free medium containing HDACi. Hypertrophy was then induced by the addition of 50 μM PE. CMs were cultured for a further 48 h before analysis. Vehicle [DMSO (dimethyl sulphoxide)] was used instead of HDACi in Control samples. Where specified, the non-specific HDACi, trichostatin A (TSA), was used as a positive control of HDAC inhibition, and the MEK-1/2 inhibitor, PD 098059 (Calbiochem), was used as a control for the inhibition of PE-induced hypertrophy.[27]

2.3.2 Western blotting

Plates were placed on ice and the CMs washed with ice-cold PBS, scraped and centrifuged. Pelleted CMs were lysed directly in Laemlli's sample buffer, boiled for 3 min, centrifuged, and loaded onto 12% SDS–PAGE. After transfer onto polyvinylidene fluoride, membranes were blocked with 5% milk tris-buffered saline-tween 20 and incubated with the following primary antibodies: anti-acetyl histone H3 and anti-histone H4 (Upstate); anti-acetyl tubulin (Sigma); anti-actin; and anti-GAPDH (glyceraldehyde-3-phosphate dehydrogenase; Chemicon). Secondary antibodies and enhanced chemiluminescence were from Amersham. For *in vivo* experiments, hearts were snap frozen in liquid N_2, pulverized with a pestle and mortar, and lysed with radio-immunoprecipitation assay buffer. Sample buffer was then added to the uncleared lysates.

2.3.3 Ribonucleic acid extraction and real-time polymerase chain reaction

For *in vitro* experiments, total ribonucleic acid (RNA) was extracted using the RNeasy mini kit (Qiagen) according to the manufacturer's instructions. The reverse transcription (RT) reaction was performed using Superscript III reverse transcriptase and random primers (Invitrogen). Real-time polymerase chain reaction (PCR) was performed in an ABI PRISM 7000 instrument (Applied Biosystems) using TaqMan technology for Caspase 3 (Casp3), atrial natriuretic factor (ANF), and skeletal actin (Sk Act), as recommended by the manufacturer.

For *in vivo* experiments, total RNA was extracted by TRIZOL (Invitrogen) according to the manufacturer's instructions. The RT reaction was then performed as the *in vitro* experiments. Real-time PCR was performed for Casp3, ANF, brain natriuretic peptide (BNP), Sk Act, and beta-myosin heavy chain (β-MHC).

To detect Casp3, Sk Act, BNP, and β-MHC, TaqMan oligonucleotides (Assay on Demand, Applied Biosystems) were used, whereas

for ANF, specific primers (For: 5′-GGA GGA GAA GAT GCC GGT AGA-3′; Rev: 5′-GCT TCC TCA GTC TGC TCA CTC A-3′) (PRIMM) and a specific probe (FAM-TGA GGT CAT GCC CCC GCA GG-TAMRA) (Applied Biosystems) were designed with the 'Primer Express' Program (Applied Biosystems).

The Assays on Demand used are given in the see Supplementary material online, *Materials and Methods*. All reactions were performed in duplicate. $2^{-\Delta\Delta CT}$ values were normalized with the values obtained for amplification of GAPDH (Assay on Demand, Applied Biosystems).

2.3.4 Morphometrical measurements

Before preparing CMs for the analyses mentioned earlier, plates were photographed under a phase contrast microscope at $\times 200$ magnification. Captured images were then analysed with Scion Image software (Scion Corp. Inc.) to obtain CM area data expressed in square pixels.

2.3.5 Immunofluorescence

Fixed CMs were stained with phalloidin-tetramethyl rhodamine iso-thiocyanate (Sigma) or anti-cardiac troponin (Chemicon) and counterstained with 4′,6-diamino-2-phenylindole (DAPI).

2.3.6 Lactate dehydrogenase release and terminal deoxynucleotidyl transferase biotin-2′-deoxyuridine 5′-triphosphate nick end labelling analysis

Culture supernatants were collected after 24 and 72 h of treatment with HDACi. Lactate dehydrogenase (LDH) released into the supernatants was quantified with the CytoTox 96® Assay Kit (Promega), following the manufacturer's indications. Supernatant from vehicle-treated CMs was used for background subtraction. Data are expressed as arbitrary units.

CMs, seeded in 24-well plates and treated as mentioned earlier, were fixed in paraformaldehyde and processed with a terminal deoxynucleotidyl transferase biotin-2′-deoxyuridine 5′-triphosphate nick end labelling (TUNEL) kit (Roche), as indicated by the manufacturer. DAPI (Sigma) was used to counterstain the nuclei. Images, captured under a fluorescence microscope, were then analysed to obtain the number of TUNEL-positive nuclei per field. A minimum of 200 cells per point were counted. Data are expressed as a percentage of DAPI-stained nuclei.

2.4 *In vivo* experimentation

This investigation conforms to the *Guide for the Care and Use of Laboratory Animals* published by the US National Institutes of Health (NIH Publication No. 85–23, revised 1996), and Italian ministerial authorization (art. 7, DL 116/92) was obtained to carry out the experimentation.

Nine-week-old female C57BL/6 mice (Charles River Laboratories) ($n = 7$ per group) were subjected to transverse aortic constriction (TAC) surgery with standard procedures and then treated intraperitoneally (i.p.) with API-D starting from day 1 after TAC. At the indicated time-points, histological, haematological, echocardiographic, and invasive haemodynamic analyses were carried out as outlined later.

2.4.1 Transverse aortic constriction

On day 0, mice were anaesthetized with a ketamine (100 mg/kg)-xylazine (2.5 mg/kg) mixture administered i.p. and then connected to a rodent ventilator after tracheal intubation.[22] The chest cavity was opened with scissors by a small incision at the level of the second intercostal space. After isolation of the aortic arch, a 7–0 silk suture was placed around the aorta and a 27–27, 5G needle. The needle was immediately removed to produce an aorta with a stenotic lumen. The chest cavity was then closed with one 6–0 nylon suture and all layers of muscle and skin closed with 6–0 continuous absorbable and nylon sutures, respectively. Sham-operated animals, which underwent surgery without the final tightening of the constrictive suture, were used as Controls.[22]

2.4.2 Administration of histone deacetylase inhibitors

Mice were treated i.p. with 3 mg/kg of API-D per day six times a week for 2 weeks, starting on day 1. This dose was found to be well tolerated. Our data also suggested that higher doses of the compound could be administered safely over prolonged periods and, as a result, we decided to use a slightly higher dose (5 mg/kg per day six times a week for 8 weeks, starting on day 1) for the long-term efficacy studies to increase the likelihood of observing effects in our functional *in vivo* readouts.

Prior to these experiments, pharmacokinetic data were generated in CD-1 mice ($n = 3$ mice evaluated per time-point). For this, API-D was solubilized in PEG400:water 1:1 and dosed at 3 mg/kg by i.p. injection. A time-course for API-D plasma concentration was also generated.

2.4.3 Echocardiographic assessment of left ventricular function

Transthoracic echocardiography was performed to evaluate left ventricular (LV) function non-invasively in isoflurane-anaesthetized closed-chest mice using a SONOS 5500 echocardiograph (Agilent Technology) fitted with an 8–15 MHz linear array transducer. LV end-systolic and end-diastolic dimensions, and wall thicknesses were evaluated by 2D M-mode as previously described.[28] Analysis was performed at the specified times before and after TAC.

2.4.4 Invasive haemodynamic assessment of cardiac function

In vivo LV function was assessed by pressure volume catheter. Mice were anaesthetized with ketamine (100 mg/kg) and xylazine (2.5 mg/kg) and connected to a rodent ventilator after endotracheal intubation. Then, bilateral vagotomy cardiac catheterization was performed using a 1.4 French (0.46 mm) conductance catheter (Scisense Inc., London, Ontario, Canada) inserted retrograde through the right carotid artery into the LV. Absolute volume was calibrated, and steady-state pressure and volume measurements were digitally recorded at 1000 (baseline). Pressure and volume measurements were also acquired during transient reduction of venous return. All experiments were carried out blind and data were analysed as previously described.[29]

2.4.5 Histology

Hearts ($n = 5$ per group) at week 4 of experimentation were quickly removed from anaesthetized mice and processed for histology using standard methods. Longitudinal sections of whole heart (4 μm thick) were stained with Masson's trichrome to evidence fibrosis. The total area affected by fibrosis in the sections obtained was quantified with image analysis software (Software NIS Elements-AR, Nikon Instruments) by two independent pathologists and expressed as μm^2.

2.5 Statistical analysis

Data are expressed as mean $\pm$ SD. Multigroup comparisons were performed using one- or two-way analysis of variance (ANOVA) with post hoc correction for multiple comparisons as appropriate. For all analyses, $P < 0.05$ was considered significant.

3. Results

To explore the effects of the HDACis selected for this study, *in vitro* experiments on neonatal rat CMs were initially performed. As HDAC suppression would be expected to induce histone hyperacetylation, due to unopposed HAT activity, we examined the acetylation status of two known HDAC targets, nuclear histone H3 and cytosolic α-tubulin, with western blotting of total cellular extracts (*Figure 1A*). HDACi was added to cultured CMs at various concentrations for 2 h and acetylation then assessed. As expected, all the

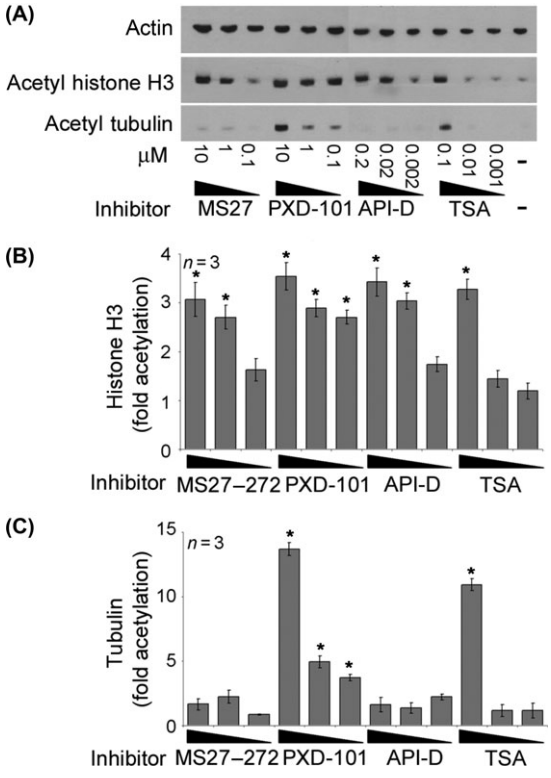

Figure 1 Dose–response relationship of the acetylation status of histone H3 and tubulin in cultured neonatal rat cardiac myocytes treated for 2 h with each of the three histone deacetylase inhibitors used in this study. (*A*) Representative western blot. (*B*) Densitometric analysis. Fold acetylation of histone H3 with respect to vehicle-treated cells (mean ± SD); $^*P < 0.05$. (*C*) Densitometric analysis. Fold acetylation of tubulin with respect to vehicle-treated cells (mean ± SD); $^*P < 0.05$, Statistical analysis was performed by one-way analysis of variance with Bonferroni post hoc correction.

HDACis used were capable of inducing a significant increase in histone H3 acetylation, thus confirming the efficacy of these inhibitors in suppressing deacetylase activity in a dose-related manner (*Figure 1B*). PXD-101, which also suppresses HDAC6 (a class II HDAC), induced a significant increase in the acetylation of α-tubulin, similarly to the broad spectrum HDACi, TSA,[30,31] whereas MS27-275 and API-D did not, in line with the notion that these two inhibitors do not affect class II HDACs at the doses used in this assay (*Figure 1C*). Blots performed at 72 h gave similar results (data not shown).

3.1 Inhibitors of class I histone deacetylases prevent cardiac myocyte hypertrophy *in vitro*

To investigate the effect on size, rat neonatal CMs were pre-treated with HDACi for 24 h and then treated with PE, a strong inducer of hypertrophy, for a further 48 h (*Figure 2A*).

Morphometric measurements indicated that treatment with inhibitors significantly blunted PE-induced hypertrophy at a concentration of 1 μM for MS27-275 and PXD-101, and 0.02 μM for API-D (*Figure 2B*). Moreover, CMs treated with HDACi showed morphological changes, probably due to the fact that these HDACis prevent sarcomere re-organization in response to hypertrophic agonists (*Figure 2C*).[11]

Expression of ANF, another parameter of CM hypertrophy, was then assessed by qRT–PCR (*Figure 2D*). The amount of ANF mRNA (messenger RNA) induced by PE treatment was significantly reduced by all HDACis, corroborating the data on cell size. PE-stimulated ANF expression was significantly inhibited at concentrations down to 0.1 μM for MS27-275 and PXD-101, and 0.002 μM for API-D; in contrast, at 10-fold lower concentrations (0.01 and 0.0002 μM, respectively for MS27-275/PXD-101 and API-D) there was little or no effect on PE-induced ANF expression, whereas ANF expression was very low at higher concentrations (10 and 2 μM for MS27-275/PXD-101 and API-D, respectively). Similar results were obtained for Sk Act gene expression (data not shown).

Time-course experiments were then performed for API-D, the most efficient drug among the three. The parameters analysed always demonstrated the efficacy of this inhibitor in reducing PE-induced hypertrophy (see Supplementary material online, *Figure S1*).

3.2 Inhibition of cardiac myocyte hypertrophy by histone deacetylase inhibitors is not due to toxicity

HDACis can induce cell death.[32] Therefore, we examined whether HDACi administration induced cytotoxicity in CMs by measuring LDH released by dying cells into the culture medium. Doses of MS27-275 up to 1 μM, PXD-101 up to 0.5 μM, and API-D up to 0.02 μM did not significantly increase LDH release after 24 h (data not shown) or 72 h of treatment (*Figure 3A*).

To evaluate potential pro-apoptotic effects of the HDACis, we analysed genomic deoxyribonucleic acid (DNA) degradation with a TUNEL assay (*Figure 3B*) and Casp3 expression with qRT–PCR (see Supplementary material online, *Figure S2*). After 72 h of treatment, doses of MS27-275 or PXD-101 up to 1 μM, and of API-D up to 0.02 μM did not increase the percentage of TUNEL-positive CMs or the expression of Casp3 mRNA.

Thus, the HDACis did not induce toxic effects within the range of concentrations observed to inhibit hypertrophy, i.e.: $\leq 1 \geq 0.01$ μM for MS27-275, $\leq 1 \geq 0.1$ μM for PXD-101, and $\leq 0.02 \geq 0.002$ μM for API-D.

3.3 An apicidin derivative attenuates cardiac hypertrophy *in vivo* and ameliorates cardiac function after pressure overload

API-D is a synthetic small-molecule derivative of the natural cyclic tetrapeptide, apicidin. We decided to use API-D to explore the efficacy in preventing cardiac hypertrophy and heart failure induced by the TAC pressure-overload model. Our choice for this compound was dictated by a series of favourable properties, i.e. good pharmacokinetics in a pre-clinical species with predicted human once-a-day oral dosing; good tolerability and efficaciousness at low doses in pre-clinical oncology models; and no off-target activities in counter screening (on 150 enzymes/receptors) ([25] and Phillip Jones *et al.*, unpublished results). These properties compare favourably with those reported for MS275, which is not tolerated well in man and has a short $T_{1/2}$,[33] and PXD-101, a hydroxamic acid with short $T_{1/2}$ and poor selectivity.[34] As a result of its molecular properties, API-D is effective at a concentration lower than other compounds, and has better pharmacokinetic properties when compared with TSA or the other HDACis tested ([25] and Phillip Jones *et al.*, unpublished results). In particular, the following pharmacokinetic data were obtained for 3 mg/kg API-D

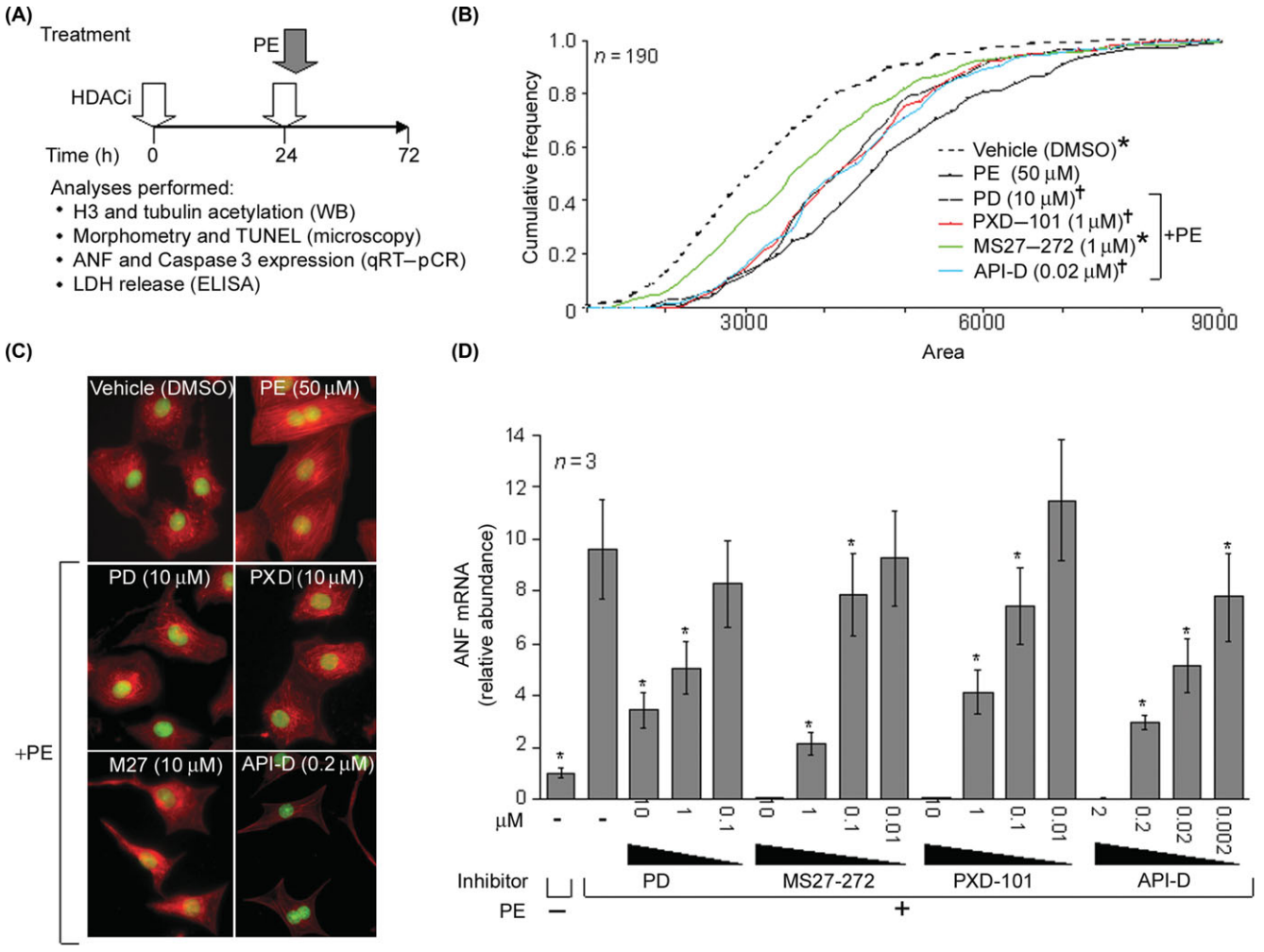

Figure 2 Treatment with histone deacetylase inhibitors significantly reduces parameters of cardiac myocyte (CM) hypertrophy *in vitro*. (*A*) Schematic of treatment protocol and analyses performed. (*B*) Representative morphometrical analysis of the cumulative frequency of CM area (given as pixels^2) after treatment at the indicated concentrations *in vitro*; *$P = 0.005$ vs. phenylephrine (PE); †$P = 0.05$ vs. PE. (*C*) Photomicrographs of CMs stained with phalloidin-tetramethyl rhodamine iso-thiocyanate (actin, in red) and DAPI (nuclei, in green). (*D*) Dose–response relationship of atrial natriuretic factor (ANF) messenger ribonucleic acid (mRNA) collected from CMs after treatment *in vitro*. Mean ± SD, normalized to glyceraldehyde-3-phosphate dehydrogenase mRNA. *$P < 0.05$ vs. PE. PE, phenylephrine; PD, PD 098059. Statistical analysis was performed by one-way analysis of variance with Bonferroni post hoc correction.

in mice: AUC = 5.7 mM.h; $C_{max} = 2.6$ mM; $T_{max} = 0.42$ h; $T_{1/2} = 2.1$ h. The time-course for plasma concentration was found to be [time (h)/concentration (mM)] 0.25/2.49, 0.5/2.27, 1/1.61, 2/0.94, 4/0.35.

Thus, 9-week-old female C57BL/6 mice were injected with API-D i.p. starting on the day after TAC, and analyses were performed as indicated (*Figure 4A*). We observed significantly lower LV and heart weight to body weight (BW) ratios in TAC-operated animals treated with API-D compared with those that were not treated; no significant differences were observed within sham groups (*Figure 4B* and see Supplementary material online, *Tables S1* and *S2*), whereas % FS (fractional shortening) did not differ between the groups (*Figure 4C*). No differences were found in terms of survival (data not shown), BW, or haematological parameters (see Supplementary material online, *Figure S3*).

Increased expression of embryonic cardiac genes (ANF, β-MHC, and Sk Act) is a hallmark of myocardial stress during pressure overload. To test whether *in vivo* API-D treatment modifies the expression of these genes, we measured the relative abundance of these mRNAs in LV extracts by qRT–PCR (*Figure 4D*). As expected, mRNA of all three genes was significantly higher in mice subjected to TAC compared with sham-operated animals ($P < 0.05$). In API-D-treated TAC-operated mice, the increase in β-MHC and Sk Act was significantly reduced. Moreover, histone H3 was more acetylated in myocardial extracts of API-D-treated animals (*Figure 4E*).

We then studied the effect of API-D on myocardial functional and biological parameters after 8 weeks of TAC, the point when mice present with a decompensated form of cardiac hypertrophy. To this end, 9-week-old female C57BL/6 mice were injected with API-D i.p. from day 1 of TAC, and analysed as outlined in *Figure 5A*. At the end of the experiment, LV/BW ratio was found significantly lower in the API-D-treated TAC-operated group than in the untreated one; no significant differences were observed between sham groups (*Figure 5B*). Other parameters of cardiac hypertrophy, such as LV mass index, diastolic interventricular septum thickness, and diastolic LV posterior wall thickness were all significantly less in the API-D-treated TAC-operated group with respect to the untreated counterpart (*Figure 5C*). LV diastolic diameter was also significantly less in TAC-operated mice when treated with

API-D. Moreover, percentage fractional shortening was significantly higher in the API-D-treated TAC-operated group with respect to the untreated TAC-operated one (*Figure 5C*).

As expected, haemodynamic evaluation showed a markedly depressed systolic function in untreated TAC-operated mice. The first derivative of LV pressure (dP/dt_{max}) was found significantly improved in the group of TAC-operated mice treated with API-D compared with the untreated counterpart (*Table 2*). Positive effects on cardiac function were confirmed also by two independent parameters of cardiac relaxation, the minimum first derivative of LV pressure (dP/dt_{min}) and exponential τ (the time constant of LV pressure decay), suggesting a better diastolic cardiac performance and, indirectly, reduced myocardial fibrosis.

In addition, a significantly lower Sk Act mRNA level was measured in the LV of the API-D-treated TAC-operated group compared with the untreated TAC-operated one (*Figure 5D*); ANF and β-MHC mRNAs were slightly reduced.

To assess whether treatment with API-D decreases fibrotic reaction, hearts were processed for histology, stained with Masson's trichrome, and the total area affected by fibrosis (i.e. stained in blue) was measured in whole-heart sections (*Figure 6*). The area of fibrosis occurring with TAC ($9.9 \times 10^6 \pm 0.8 \times 10^6\ \mu m^2$) was significantly (two-way ANOVA with Bonferroni post-test, $P < 0.05$) reduced by treatment with API-D ($5.5 \times 10^6 \pm 0.5 \times 10^6 \mu m^2$).

No differences were found between the untreated and API-D-treated sham-operated groups in terms of survival, Casp3 expression (measured by qRT–PCR on RNA samples extracted from LV tissue), and BW (see Supplementary material online, *Tables S1* and *S2*). Moreover, haematological parameters were within the norm for all groups (see Supplementary material online, *Figure S4*).

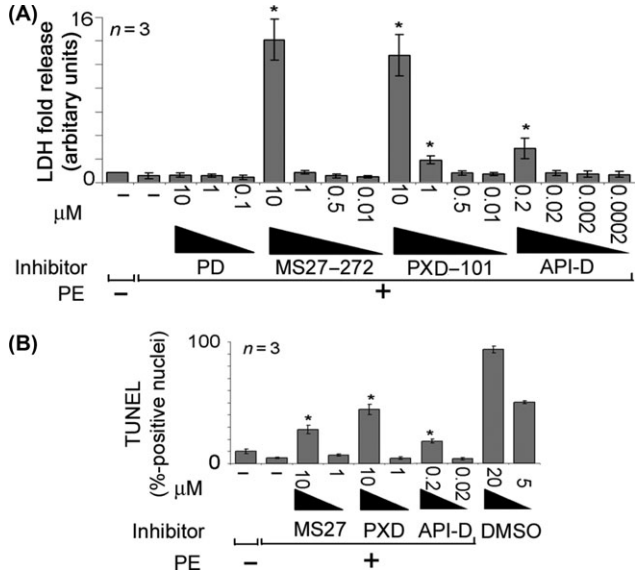

Figure 3 Analysis of cell death. (*A*) Dose–response of lactate dehydrogenase (LDH) released into the medium by cardiac myocytes (CMs) treated *in vitro*. Mean ± SD. *$P < 0.05$ vs. phenylephrine (PE). (*B*) Terminal deoxynucleotidyl transferase biotin-2′-deoxyuridine 5′-triphosphate nick end labelling (TUNEL) analysis of apoptosis. Dimethyl sulphoxide (DMSO) was used as a positive control at concentrations of 5 and 20%. *$P < 0.05$ vs. PE. PE, phenylephrine; PD, PD 098059. Statistical analysis was performed by one-way analysis of variance with Bonferroni post hoc correction.

4. Discussion

We have focused on the characterization of new HDAC inhibitors, describing an apidicin derivative with a specific HDAC class I inhibiting activity in particular. API-D is part of a structurally novel family of HDAC inhibitors since it

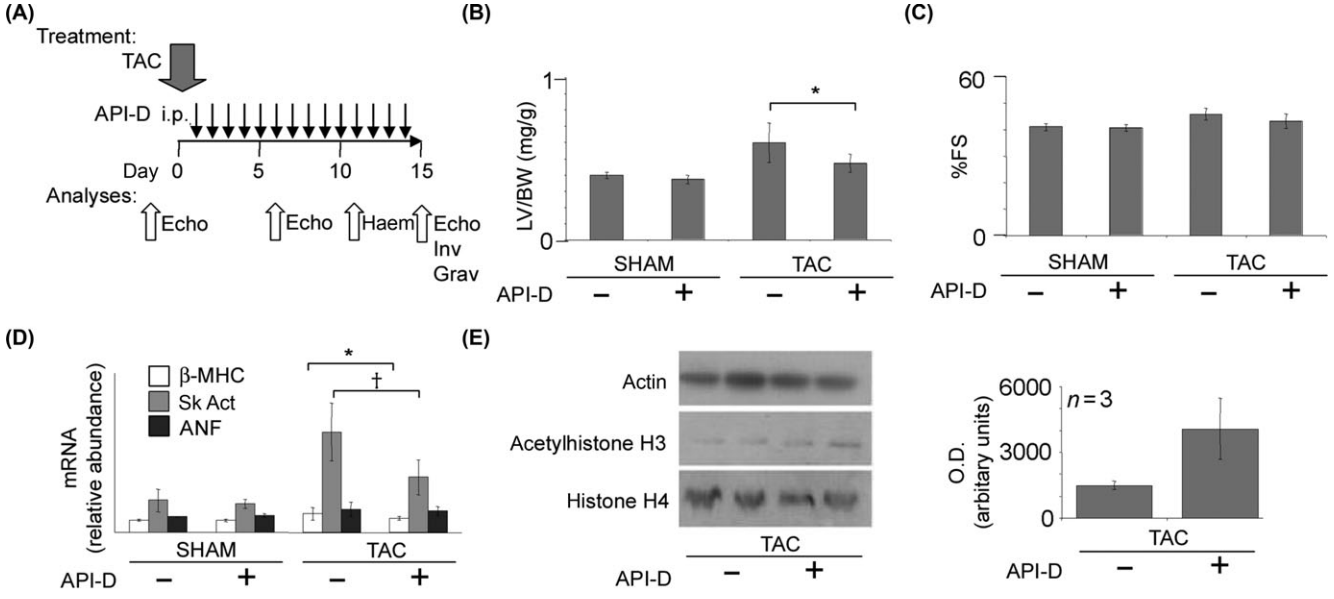

Figure 4 *In vivo* administration of apicidin derivative (API-D) blunts pressure overload-induced cardiac hypertrophy. (*A*) Schematic of the treatment protocol and analyses performed in the short-term *in vivo* study. TAC, transverse aortic constriction; Echo, echocardiography; Inv, invasive haemodynamical analysis; Grav, gravitometrical measurements. (*B*) Graph of left ventricle (LV) weight to body weight (BW) ratio. Within the TAC-operated groups, the ratio increased significantly less when API-D was administered. *$P < 0.001$ [two-way analysis of variance (ANOVA)]. (*C*) Graph of fractional shortening. (*D*) Foetal gene messenger ribonucleic acid (mRNA) expression was evaluated in LV by qRT–PCR (quantitative reverse transcription polymerase chain reaction) (mean ± SD, normalized to glyceraldehyde-3-phosphate dehydrogenase mRNA). β-MHC, beta-myosin heavy chain; ANF, atrial natriuretic factor; Sk Act, skeletal actin; *$P < 0.04$; †$P = 0.02$ (two-way ANOVA). (*E*) Representative western blot of histone H3 acetylation status in total extracts of LV tissue obtained from TAC-operated mice with and without API-D treatment (left). Densitometric analysis (right).

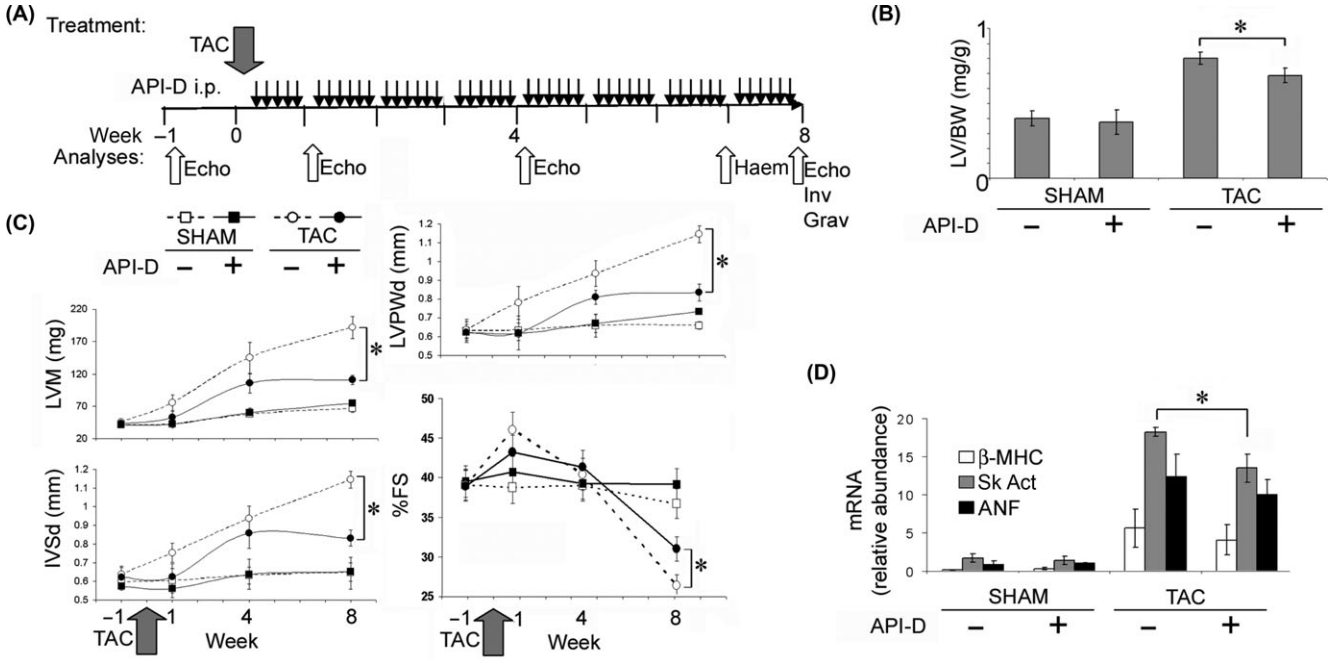

Figure 5 *In vivo* administration of apicidin derivative (API-D) preserves cardiac function in the long-term. (*A*) Schematic of treatment protocol and analyses performed for the long-term experiments. TAC, transverse aortic constriction; Echo, echocardiography; Inv, invasive haemodynamical analysis; Grav, gravitometrical measurements. (*B*) Left ventricle (LV) weight to body weight (BW) ratio. *$P < 0.001$ [two-way analysis of variance (ANOVA)]. (*C*) Time-course of % fractional shortening (FS), LV mass (LVM), diastolic interventricular septal thickness (IVSd), and diastolic LV posterioral wall thickness (LVPWd) for each group. *$P = 0.05$ (two-way ANOVA). (*D*) Foetal gene messenger ribonucleic acid (mRNA) expression evaluated by qRT–PCR (quantitative reverse transcription polymerase chain reaction) (mean ± SD, normalized to glyceraldehyde-3-phosphate dehydrogenase mRNA). *$P < 0.01$ (two-way ANOVA).

Table 2 Haemodynamic parameters in mice after 8 weeks of treatment

	Control ($n = 6$)	TAC ($n = 6$)	TAC + API-D ($n = 5$)
P–V loop analysis			
Heart rate (bpm)	249 ± 13	317 ± 27[a]	324 ± 28[a]
End-systolic volume (μL)	12.4 ± 0.3	22.2 ± 5.4[a]	15.5 ± 4.0
End-diastolic Volume (μL)	25.8 ± 1.9	29.2 ± 4.2[a]	26.1 ± 4.9
Elastic Elastance (Ea) (mmHg/μL)	6.7 ± 1.2	23.3 ± 6.2[a]	17.9 ± 1.5[a]
Systolic function			
Maximum Pressure (mmHg)	80.5 ± 2.9	112.1 ± 14.6[a]	121.7 ± 16.2[a]
End-systolic Pressure (mmHg)	77.4 ± 2.2	110.2 ± 14.2[a]	115.0 ± 17.5[a]
d*P*/d*t* max (mmHg/s)	4485 ± 133	3405 ± 501[a]	4776 ± 514[b]
Ejection Fraction (%)	55.4 ± 1.6	24.6 ± 2.0[a]	41.6 ± 6.0[a,b]
Stroke Volume (μL)	13.0 ± 2.4	7,0 ± 2.2[a]	12.1 ± 2.5[a,b]
Cardiac Output (mL/min)	3.2 ± 0.7	2.1 ± 0.5[a]	3.7 ± 0.6[b]
E_{es}	8.5 ± 1.3	1.5 ± 1.0[a]	11.6 ± 0.9[a,b]
E_{max}	12.5 ± 0.6	8.1 ± 2.3[a]	15.2 ± 0.6[b]
Diastolic function			
End-diastolic Pressure (mmHg)	9.0 ± 2.0	15.0 ± 3.2[a]	10.0 ± 4.0[b]
d*P*/d*t* min (mmHg/s)	−3566 ± 305	−2989 ± 496[a]	−4183 ± 550[b]
τ_w (ms)	12.5 ± 0.9	18.6 ± 3.6[a]	13.1 ± 1.6[b]
slope-EDPVR	0.5 ± 0.3	0.8 ± 0.2[a]	1.0 ± 0.4[a]

[a]$P < 0.05$ vs. Control; [b]$P < 0,05$ vs. TAC. Comparisons were made using ANOVA with Neuman–Keuls correction.

neither contains a hydroxamic acid (as does PXD-101) nor a benzamide moiety (as does MS27-275), but it is thought to bind to the HDAC active site Zn^{+} ion via a hydrated ketone group.[25] Our data demonstrate that the use of this compound blunts hypertrophic cardiac growth in mice and, thus, has positive effects on heart failure progression without producing any obvious side effects.

Cardiac myocytes (CM) respond to stress by activating gene expression programs. Many transcription factors have been identified that are critical for the induction of specific genes activated during hypertrophy.[35] The post-genomic era, however, has shown that transcription factors are not the unique key regulators of gene expression. Epigenetic mechanisms such as DNA methylation, post-translational

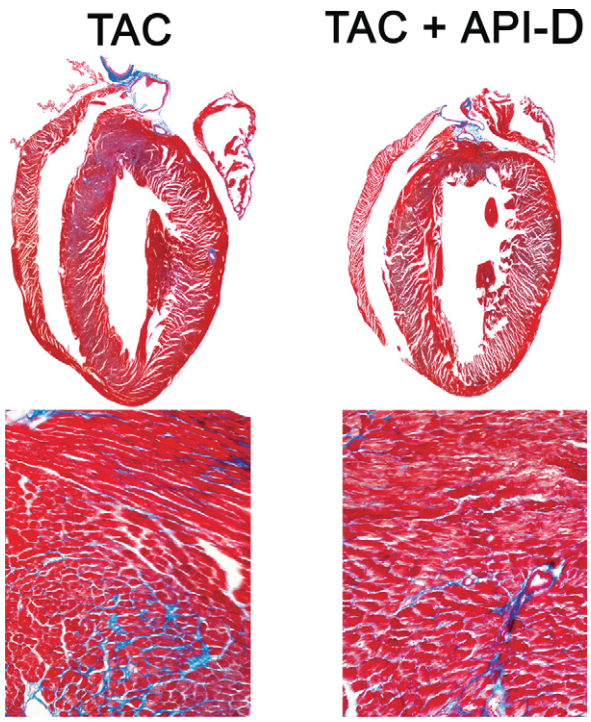

Figure 6 Apicidin derivative (API-D) reduces fibrosis of hearts subjected to transverse aortic constriction (TAC). Representative sections of whole mouse heart subjected to TAC (left) and TAC + API-D (right) for 4 weeks and stained with Masson's trichrome to evidence fibrosis. Staining for fibrosis (blue) seen in the ventricle walls of TAC-only mice was reduced by the administration of API-D (×2.5). Bottom, enlarged portion of heart from a TAC (left) and TAC + API-D (right) mouse (×20).

modifications of histone proteins, remodelling of nucleosomes, and expression of small regulatory RNAs all contribute to regulation of gene expression and determination of cell and tissue specificity. These mechanisms are reversible and represent potential targets for therapeutic intervention. The regulation of gene expression through histone acetylation has been demonstrated to be particularly relevant and complex for CM growth and myocardial hypertrophy.[13,36,37]

Class I and class II HDACs seem to have opposite effects on hypertrophic pathways. Class II HDACs repress hypertrophy,[9,38] whereas class I HDACs are required for some aspects of the hypertrophic response. Inhibitors that block the catalytic activity of both class I and class II HDACs prevent hypertrophic responses in both isolated myocytes and intact mice, suggesting that the predominant targets of these chemical inhibitors are class I HDACs.[11,39] Recently, it was proposed that HDAC2, among the class I HDACs, is a major target of HDAC inhibitors in the heart, indicating this HDAC as a target for the treatment of cardiac hypertrophy and heart failure.[14] Knockout of HDAC2 was demonstrated to increase expression of the gene encoding inositol polyphosphate-5-phosphatase f, resulting in constitutive activation of glycogen synthase kinase-3beta via inactivation of Akt and 3-phosphoinositide-dependent protein kinase-1.[14] Inhibition of cardiac hypertrophy *in vivo* by either generic or class I-specific HDAC inhibitors was found to improve cardiac function and blunt fibrosis significantly.[12,40] Overall, our data obtained with the novel compound, API-D, together and in agreement with the literature suggest that the beneficial effect of HDAC inhibition includes attenuation of fibrosis and reduced switching of contractile protein isoforms.

We acknowledge the limitations of our study in that it is relatively underpowered and that it does not compare *in vivo* all the inhibitors used in the study, but the functional improvement seen in the mice was found to be significant with relatively low doses of API-D. The small but significant blunting of hypertrophy produced with this compound may not explain the improved heart function totally, and as yet unknown mechanisms, apart from transcriptional-related ones, might be involved. On this point, a very recent report has revealed that HDACs influence cardiac function at an extra-nuclear level:[41] treatment of cardiomyocytes with HDAC inhibitors results in an increased acetylation of sarcomeric proteins that enhances myofilament calcium sensitivity. Muscle LIM protein—the cytosolic target of HDAC4, a class II HDAC, and PCAF, a HAT—was found to be central to this mechanism. Thus, protein acetylation is another layer of regulation controlling muscle physiology that might be targeted when using HDAC inhibitors; we do not exclude the possibility that API-D might also affect cardiac function through altered acetylation of sarcomeric proteins, perhaps indirectly through an effect mediated by class II HDACs. In fact, in that report, the class I HDAC inhibitor, MS275, was found to have an effect that was comparable with that of the generic HDAC inhibitors, TSA and scriptaid.

Despite *in vitro* data, which clearly demonstrate reduced expression of hypertrophy markers, data obtained *in vivo* can be more difficult to interpret. In fact, the expression of ANF *in vivo* has been reported to be profoundly affected in one instance,[40] whereas in another report the effect of HDAC inhibition on ANF expression was limited.[12] We observed *in vivo* that the ANF transcript level was increased in API-D-treated TAC-operated mice to a similar extent as untreated TAC-operated mice even if hypertrophy was significantly blunted in the former; on the other hand, β-MHC and Sk Act were reduced. E. Olson's lab reported a similar discrepancy between *in vitro* and *in vivo* ANF levels after the use of TSA.[11,12] An enhancement of gene expression in general is a consequence of HDAC inhibition; therefore, generic transcriptional effects could a be reason for confounding mRNA expression levels *in vivo*.

Dissection of the mechanisms underlying HDAC inhibition represents a continuing challenge in cardiology. In oncology, these drugs are already under clinical trials for the treatment of cancer. Because class I HDAC inhibition prevents cardiac hypertrophy induced by pressure overload and greatly improves heart function, HDAC inhibitory compounds hold promise to be a new pharmacologic tool also for the treatment of heart failure.

Supplementary material

Supplementary material is available at *Cardiovascular Research* online.

Funding

Italian Ministry of University and Research; Italian Ministry of Health; European Community EU Framework Programme 6 (LSHM-CT-2005-018833, EUGeneHeart) to G.C.

Acknowledgements

We are grateful to Angela Pitisci for technical help and Dr Natalia Rivera for statistical analysis.

Conflict of interest: P.G., P.J., P.G., R.De F., G.C. and C.S. are employees of Merck & Co Inc.

References

1. Thiagalingam S, Cheng KH, Lee HJ, Mineva N, Thiagalingam A, Ponte JF. Histone deacetylases: unique players in shaping the epigenetic histone code. *Ann NY Acad Sci* 2003;**983**:84–100.
2. Acharya MR, Sparreboom A, Venitz J, Figg WD. Rational development of histone deacetylase inhibitors as anticancer agents: a review. *Mol Pharmacol* 2005;**68**:917–932.
3. Butler LM, Agus DB, Scher HI, Higgins B, Rose A, Cordon-Cardo C *et al*. Suberoylanilide hydroxamic acid, an inhibitor of histone deacetylase, suppresses the growth of prostate cancer cells in vitro and in vivo. *Cancer Res* 2000;**60**:5165–5170.
4. Gray SG, Ekstrom TJ. The human histone deacetylase family. *Exp Cell Res* 2001;**262**:75–83.
5. Marmorstein R. Structure of histone deacetylases: insights into substrate recognition and catalysis. *Structure* 2001;**9**:1127–1133.
6. Verdin E, Dequiedt F, Kasler HG. Class II histone deacetylases: versatile regulators. *Trends Genet* 2003;**19**:286–289.
7. Gregoretti IV, Lee YM, Goodson HV. Molecular evolution of the histone deacetylase family: functional implications of phylogenetic analysis. *J Mol Biol* 2004;**338**:17–31.
8. Imai S, Armstrong CM, Kaeberlein M, Guarente L. Transcriptional silencing and longevity protein Sir2 is an NAD-dependent histone deacetylase. *Nature* 2000;**403**:795–800.
9. Zhang CL, McKinsey TA, Chang S, Antos CL, Hill JA, Olson EN. Class II histone deacetylases act as signal-responsive repressors of cardiac hypertrophy. *Cell* 2002;**110**:479–488.
10. Gusterson RJ, Jazrawi E, Adcock IM, Latchman DS. The transcriptional co-activators CREB-binding protein (CBP) and p300 play a critical role in cardiac hypertrophy that is dependent on their histone acetyltransferase activity. *J Biol Chem* 2003;**278**:6838–6847.
11. Antos CL, McKinsey TA, Dreitz M, Hollingsworth LM, Zhang CL, Schreiber K *et al*. Dose-dependent blockade to cardiomyocyte hypertrophy by histone deacetylase inhibitors. *J Biol Chem* 2003;**278**:28930–28937.
12. Kong Y, Tannous P, Lu G, Berenji K, Rothermel BA, Olson EN *et al*. Suppression of class I and II histone deacetylases blunts pressure-overload cardiac hypertrophy. *Circulation* 2006;**113**:2579–2588.
13. Backs J, Olson EN. Control of cardiac growth by histone acetylation/deacetylation. *Circ Res* 2006;**98**:15–24.
14. Trivedi CM, Luo Y, Yin Z, Zhang M, Zhu W, Wang T *et al*. Hdac2 regulates the cardiac hypertrophic response by modulating Gsk3 beta activity. *Nat Med* 2007;**13**:324–331.
15. Lowes BD, Gilbert EM, Abraham WT, Minobe WA, Larrabee P, Ferguson D *et al*. Myocardial gene expression in dilated cardiomyopathy treated with beta-blocking agents. *N Engl J Med* 2002;**346**:1357–1365.
16. Harding VB, Jones LR, Lefkowitz RJ, Koch WJ, Rockman HA. Cardiac beta ARK1 inhibition prolongs survival and augments beta blocker therapy in a mouse model of severe heart failure. *Proc Natl Acad Sci USA* 2001;**98**:5809–5814.
17. Rockman HA, Chien KR, Choi DJ, Iaccarino G, Hunter JJ, Ross J Jr *et al*. Expression of a beta-adrenergic receptor kinase 1 inhibitor prevents the development of myocardial failure in gene-targeted mice. *Proc Natl Acad Sci USA* 1998;**95**:7000–7005.
18. Antos CL, McKinsey TA, Frey N, Kutschke W, McAnally J, Shelton JM *et al*. Activated glycogen synthase-3 beta suppresses cardiac hypertrophy in vivo. *Proc Natl Acad Sci USA* 2002;**99**:907–912.
19. Rothermel BA, McKinsey TA, Vega RB, Nicol RL, Mammen P, Yang J *et al*. Myocyte-enriched calcineurin-interacting protein, MCIP1, inhibits cardiac hypertrophy in vivo. *Proc Natl Acad Sci USA* 2001;**98**:3328–3333.
20. Hill JA, Karimi M, Kutschke W, Davisson RL, Zimmerman K, Wang Z *et al*. Cardiac hypertrophy is not a required compensatory response to short-term pressure overload. *Circulation* 2000;**101**:2863–2869.
21. Shimoyama M, Hayashi D, Takimoto E, Zou Y, Oka T, Uozumi H *et al*. Calcineurin plays a critical role in pressure overload-induced cardiac hypertrophy. *Circulation* 1999;**100**:2449–2554.
22. Esposito G, Rapacciuolo A, Naga Prasad SV, Takaoka H, Thomas SA, Koch WJ *et al*. Genetic alterations that inhibit in vivo pressure-overload hypertrophy prevent cardiac dysfunction despite increased wall stress. *Circulation* 2002;**105**:85–92.
23. Saito A, Yamashita T, Mariko Y, Nosaka Y, Tsuchiya K, Ando T *et al*. A synthetic inhibitor of histone deacetylase, MS-27–275, with marked in vivo antitumor activity against human tumors. *Proc Natl Acad Sci USA* 1999;**96**:4592–4597.
24. Plumb JA, Finn PW, Williams RJ, Bandara MJ, Romero MR, Watkins CJ *et al*. Pharmacodynamic response and inhibition of growth of human tumor xenografts by the novel histone deacetylase inhibitor PXD101. *Mol Cancer Ther* 2003;**2**:721–728.
25. Jones P, Altamura S, Chakravarty PK, Cecchetti O, De Francesco R, Gallinari P *et al*. A series of novel, potent, and selective histone deacetylase inhibitors. *Bioorg Med Chem Lett* 2006;**16**:5948–5952.
26. Condorelli G, Drusco A, Stassi G, Bellacosa A, Roncarati R, Iaccarino G *et al*. Akt induces enhanced myocardial contractility and cell size in vivo in transgenic mice. *Proc Natl Acad Sci USA* 2002;**99**:12333–12338.
27. Alessi DR, Cuenda A, Cohen P, Dudley DT, Saltiel AR. PD 098059 is a specific inhibitor of the activation of mitogen-activated protein kinase kinase in vitro and in vivo. *J Biol Chem* 1995;**270**:27489–27494.
28. Tanaka N, Dalton N, Mao L, Rockman HA, Peterson KL, Gottshall KR *et al*. Transthoracic echocardiography in models of cardiac disease in the mouse. *Circulation* 1996;**94**:1109–1117.
29. Perrino C, Naga Prasad SV, Mao L, Noma T, Yan Z, Kim HS *et al*. Intermittent pressure overload triggers hypertrophy-independent cardiac dysfunction and vascular rarefaction. *J Clin Invest* 2006;**116**:1547–1560.
30. Hubbert C, Guardiola A, Shao R, Kawaguchi Y, Ito A, Nixon A *et al*. HDAC6 is a microtubule-associated deacetylase. *Nature* 2002;**417**:455–458.
31. Brush MH, Guardiola A, Connor JH, Yao TP, Shenolikar S. Deactylase inhibitors disrupt cellular complexes containing protein phosphatases and deacetylases. *J Biol Chem* 2004;**279**:7685–7691.
32. Marks PA, Richon VM, Rifkind RA. Histone deacetylase inhibitors: inducers of differentiation or apoptosis of transformed cells. *J Natl Cancer Inst* 2000;**92**:1210–1216.
33. Ryan QC, Headlee D, Acharya M, Sparreboom A, Trepel JB, Ye J *et al*. Phase I and pharmacokinetic study of MS-275, a histone deacetylase inhibitor, in patients with advanced and refractory solid tumors or lymphoma. *J Clin Onc* 2005;**23**:3912–3922.
34. Warren KE, McCully C, Dvinge H, Tjørnelund J, Sehested M, Lichenstein HS *et al*. Plasma and cerebrospinal fluid pharmacokinetics of the histone deacetylase inhibitor, belinostat (PXD101), in non-human primates. *Cancer Chemother Pharmacol* 2008;**62**:433–437.
35. Frey N, Olson EN. Cardiac hypertrophy: the good, the bad, and the ugly. *Annu Rev Physiol* 2003;**65**:45–79.
36. McKinsey TA, Olson EN. Cardiac histone acetylation – therapeutic opportunities abound. *Trends Genet* 2004;**20**:206–213.
37. McKinsey TA, Olson EN. Toward transcriptional therapies for the failing heart: chemical screens to modulate genes. *J Clin Invest* 2005;**115**:538–546.
38. Chang S, McKinsey TA, Zhang CL, Richardson JA, Hill JA, Olson EN. Histone deacetylases 5 and 9 govern responsiveness of the heart to a subset of stress signals and play redundant roles in heart development. *Mol Cell Bio* 2004;**24**:8467–8476.
39. Kook H, Lepore JJ, Gitler AD, Lu MM, Wing-Man Yung W, Mackay J *et al*. Cardiac hypertrophy and histone deacetylase-dependent transcriptional repression mediated by the atypical homeodomain protein Hop. *J Clin Invest* 2003;**112**:863–871.
40. Kee HJ, Sohn IS, Nam KI, Park JE, Qian YR, Yin Z *et al*. Inhibition of histone deacetylation blocks cardiac hypertrophy induced by angiotensin II infusion and aortic banding. *Circulation* 2006;**113**:51–59.
41. Gupta MP, Samant SA, Smith SH, Shroff SG. HDAC4 and PCAF bind to cardiac sarcomeres and play a role in regulating myofilament contractile activity. *J Biol Chem* 2008;**283**:10135–10146.